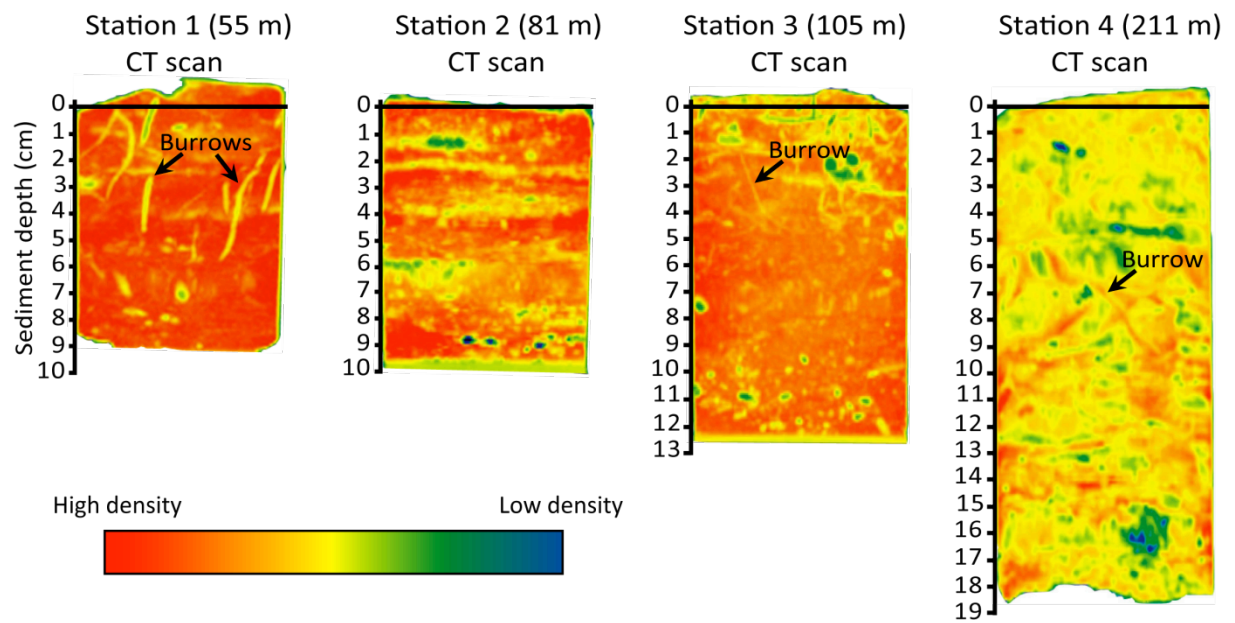


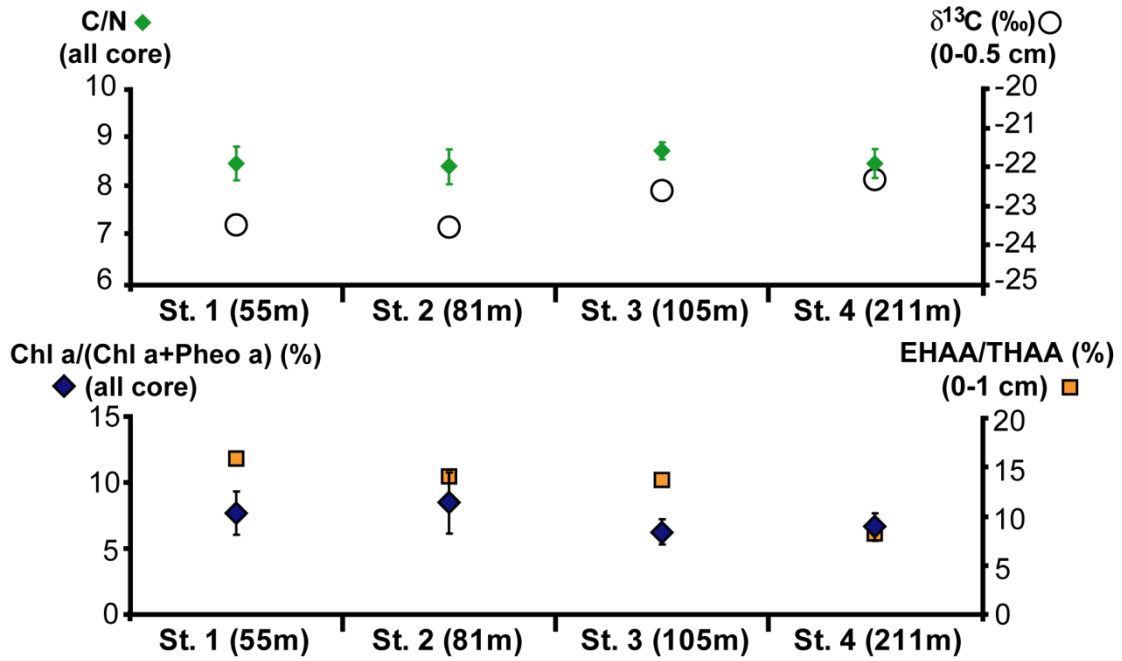
**Unexpected biotic resilience on the Japanese seafloor caused by the 2011 Tōhoku-Oki  
tsunami - supplementary information**

Takashi Toyofuku, Pauline Duros, Christophe Fontanier, Briony Mamo, Sabrina Bichon,  
Roselyne Buscail, Gérard Chabaud, Bruno Deflandre, Sarah Goubet, Antoine Grémare,  
Christophe Menniti, Minami Fujii, Kiichiro Kawamura, Karoliina Annika Koho, Atsushi  
Noda, Yuichi Namegaya, Kazumasa Oguri, Olivier Radakovitch, Masafumi Murayama,  
Lennart Jan de Nooijer, Atushi Kurasawa, Nina Ohkawara, Takashi Okutani, Arito Sakaguchi,  
Frans Jorissen, Gert-Jan Reichart and Hiroshi Kitazato

**Figure S1.** CT-scan images of sediment cores at the four stations.



**Figure S2.** Description of sedimentary organic matter ( $\delta^{13}\text{C}$ , C/N atomic ratio, [Chl *a*/(Chl *a*+Pheo *a*)] ratio in %, [EHAA/THAA] ratio in %) at the four stations.



## **Detailed Methods**

### *Sampling*

Sediment samples were collected with a Barnett-type multi-corer equipped with 8 PCPE tubes (82 mm internal diameter)<sup>1</sup>. The multi-corer allowed sampling of the uppermost centimeters of the sediment column, the overlying bottom waters, and a comparatively undisturbed sediment-water interface. It was deployed once at Stations 1-3, and twice at Station 4. In the later case, two cores were dedicated to radionuclide (total <sup>210</sup>Pb) analysis and CT-Scan treatments were gathered on the second deployment. At Stations 1, 2 and 3, all cores processed for this study were taken from the single deployment. At each station, a first core was sliced horizontally every 0.5 cm from the sediment-water interface to 4 cm depth, every 1cm between 4 and 6cm and then every 2-cm down to 10 cm. Each sediment slice was divided into four subsamples and immediately frozen (-80°C) on board. Back at the laboratory, three samples were freeze-dried and assessed for sedimentary organic matter (C/N atomic ratio,  $\delta^{13}\text{C}$  in organic carbon, amino acids) and grain-size analysis. The 4th subsample was stored at -80°C until chlorophyllic pigment analysis. Note that  $\delta^{13}\text{C}$  was analyzed only in the first half centimeter whereas amino acids were processed in the first centimeter of sediment. Another core per station was processed for foraminiferal investigation.

### *Geochemical Analysis - Organic Matter Analyses*

Total nitrogen, total and organic carbon concentrations (TN and TOC, respectively) were measured using freeze-dried sediment subsamples (~280 mg DW). Homogenized, weighted samples were analyzed in an automatic CN-analyzer Elementar VarioMax, after acidification with 2M HCl (40°C overnight) to remove carbonates. Precision measurements were about 2% and 0.3% DW for TN and OC, respectively. Stable carbon isotopes ( $\delta^{13}\text{C}$ ) were measured on samples treated with HCl (2M) to remove carbonate and then, subsequently rinsed with cold

deionized water to remove chloride before freeze-drying<sup>2</sup>. A few milligrams of the powdered material were loaded into tin cups and placed in the automated sample carousel of the elemental analyzer (EA 3000 Eurovector) coupled with an Isotopic Ratio Mass Spectrometer (IR/MS, GVI Isoprime). The standard deviation for replicates of internal standards is better than  $\pm 0.2$  ‰ for isotopic ratios.

Total hydrolysable amino acids (THAA) and enzymatically hydrolysable amino acids (EHAA) were assessed in the first centimeter of the freeze-dried sediment subsamples. Bulk sediment was first crushed and passed through a 200 $\mu$ m mesh. THAA and EHAA were assayed from work established by others<sup>3</sup>. Approximately 15 mg DW of sediment were mixed with 500  $\mu$ L of 6M HCl (100°C) for 24 hours under vacuum. Hydrolysed subsamples (100  $\mu$ L) were neutralized with 100  $\mu$ L of 6M NaOH, and buffered with 2 mL of H<sub>3</sub>BO<sub>3</sub> (0.4 M, pH = 10). Fluorescent derivatives were obtained by adding 200  $\mu$ L of an orthophthaldialdehyde (OPA) solution (100 mg OPA/1 mL methanol, 100 mL buffer pH = 9.8 and 0.05 mL mercaptoethanol) and 2 mL of phosphate buffer (pH = 8) to 200  $\mu$ L of those samples. Total hydrolysable amino acids were quantified 2 minutes 30 seconds after OPA addition through fluorescence measurements (Excitation wavelength 340 nm and emission wavelength 453 nm; Perkin Elmer LS55 fluorescence spectrometer). Enzymatically hydrolysable amino acids (EHAA) were extracted following a biomimetic approach<sup>3</sup>. Approximately 100 mg of DW sediment were poisoned with a 1mL solution containing sodium arsenate (0.1 M) and pentachlorophenol (0.1 mM) within a sodium phosphate buffer (pH = 8), and were incubated for 1 hour at room temperature to prevent the bacterial utilization of amino acids released after the addition of 100  $\mu$ L of proteinase K solution (1 mg/mL). Sediment was then incubated for 6 hours at 37°C. After centrifugation, 75  $\mu$ L of pure trichloroacetic acid were added to 750  $\mu$ L of supernatant to precipitate macromolecules, which are considered to be unsuitable for absorption. After another centrifugation, 750  $\mu$ L of the supernatant was hydrolyzed and

processed as described for THAA. A blank accounting for possible degradation of the enzyme was carried out. Enzymatically hydrolysable amino acids were then quantified using the procedure described above for THAA. The EHAA/THAA ratios (expressed in %) were computed for each station<sup>4-6</sup>. This ratio is indicative of the lability of amino acids. For chlorophyll *a* and pheophytin *a*, frozen (-80°C) sediment subsamples (between 0.5 and 3.7 g) were extracted (overnight, 4°C) with 90% acetone (final concentration taking into account sediment water content). They were then centrifuged and their supernatant was used to assess chlorophyll *a* and pheophytin *a*<sup>7</sup>. The [Chl *a*/(Chl *a* + Pheo *a*)] ratios (expressed in %) were computed in percentage for each station. This ratio is indicative of the freshness of plant material.

### *Sediment Properties*

#### Grain-size analysis

Grain-size was analyzed using a Malvern® Laser Diffraction Particle Size. Before analytic processes, bulk (not decarbonated) sediments were drowned in water and moderately stirred with a plastic probe. Grain-size values are expressed in the 10<sup>th</sup> and the 90<sup>th</sup> percentiles (D<sub>10</sub> and D<sub>90</sub> respectively).

#### Total <sup>210</sup>Pb Radionuclide Activity

At each station, the sediment core dedicated to radionuclide was sliced horizontally every 0.5 cm from the sediment-water interface to 4 cm depth, every 1 cm between 4 and 6 cm depth and then every 2 cm down to the bottom of the sediment column. Sediment samples were stored in plastic bags at ambient temperature. Radionuclide activities at Station 2 were measured at JAMSTEC (Japan). Sediment samples were transferred into plastic cubes in constant volume to measure water contents. After measuring the total weight, the plastic

cubes with the sediments were put in an oven at 80°C and left for two days. Then, dry weight was measured and the sediments were subsequently ground in a mortar. Two grams of powdered samples were transferred to plastic tubes and sealed hermetically. The samples were left for more than two months to wait for secular equilibrium between  $^{226}\text{Ra}$  and  $^{222}\text{Rn}$ . Gamma-ray spectra were measured with a gamma-ray analysis system equipped by SEIKO EG&G consisting of an ORTTEC 12030 well type germanium detector and a MCA-7800 spectrum analyzer. The peak areas of  $^{210}\text{Pb}$  (46.5 keV) were calculated by Gaussian curve fitting using a KaleidaGraph 4.1 software (Synergy Software, USA). Radionuclide activities were quantified and corrected for their respective counting efficiencies as determined by standard materials (CANMET DL-1a uranium-thorium ore). Applied counting times ranged from one to three days.  $^{210}\text{Pb}$  activities of cores gathered at Stations 1, 3 and 4 were measured by alpha spectrometry of its granddaughter  $^{210}\text{Po}$  at the CEREGE laboratory (France). Immediately after the cruise, wet sediment samples were transported back to France and dried in the laboratory. Samples were dissolved in a mixture of HCl, HNO<sub>3</sub> and HF in the presence of  $^{209}\text{Po}$  as a yield tracer. Po was plated spontaneously from 1.5N HCl solution onto Ag disks. Uncertainties were calculated by standard propagation of the 1 sigma counting errors of samples and blanks.

#### Lithological description, Mineralogy and CT-Scan

Collected sediment cores were refrigerated on board. In the laboratory, X-ray CT images were taken by a CT scanner equipped in the Center for Advanced Marine Core Research, Kochi University (Pratico, Hitachi, Japan). After the scanning, the cores were split vertically and one section was used for lithology descriptions. Microscopic smear slide observations were carried using a polarized light microscope (CX31P, Olympus, Japan).

### Benthic Foraminiferal Analysis

One core per station gathered on the 1<sup>st</sup> multi-corer deployment was sliced horizontally every 0.5 cm from the sediment-water interface to 4 cm depth, every 1 cm between 4–6 cm depth and then every 2 cm down to 10 cm. Corresponding samples were transferred on board in 500 cm<sup>3</sup> bottles, which were filled with 95% ethanol containing 1g/L Rose Bengal stain, commonly used to identify live foraminifera<sup>8,9</sup>. All samples were gently shaken for several minutes to obtain a homogeneous mixture. Back at the laboratory, they were sieved through both 63µm and 150µm screens and the sieve residues were stored in 95% ethanol. Stained foraminifera belonging to the larger size fraction (>150 µm) were sorted in wet samples and stored in Plummer slides. One problem with this technique is that Rose Bengal may stain the protoplasm of dead foraminifera, which may be relatively well-preserved for long time periods under the anoxic conditions that generally prevail in deep sediments<sup>10,11</sup>. We therefore applied very strict staining criteria (i.e., all chambers except the last one stained bright pink), and compared doubtful individuals to perfectly stained ones of the same species found in superficial sediment layers. Non-transparent agglutinated and miliolid taxa were broken on many occasions for inspection of the interior of the test. Most stained foraminifera were identified at species level (see Appendix 1 for census data including taxonomic lists). Because samples were preserved and sorted in ethanol, many soft-shelled foraminiferal species may have shrunk and become unrecognizable during picking. Thus, our counts probably underestimate the soft-shelled foraminiferal group. At each station, we calculated sample diversity (S) representing the number of taxa (identified at least to the genus level). As an information statistic index, we also calculated the Shannon Index (H') as described in Murray<sup>12</sup>.

### *Modelisation*

### Tsunami simulation

For numerical simulation of the 2011 Tōhoku-Oki Tsunami propagation, the non-linear shallow-water equations and the equation of continuity on the Cartesian coordinate system are solved by using a finite difference method<sup>13</sup>. The coefficient of the bottom friction or Manning's roughness coefficient is set at  $0.03 \text{ m}^{-1/3}\text{s}$ . In the deep ocean outside the source area, the nonlinear advection terms and the bottom friction term are neglected. Total reflection is assumed at the coast, and radiation condition is set on the boundary to the outer sea. The computation area is approximately from  $139^\circ\text{E}$  to  $147^\circ\text{E}$  and  $35^\circ\text{N}$  to  $44^\circ\text{N}$ . The grid sizes of the coarsest 2025 m and finest 225 m are adopted. Stations 1-4, where the velocity is calculated, are inside the 225 m grid-size area. The time interval of the computation is 0.5 s, and the tsunami propagation is during the six hours after the mainshock. For the initial condition, the spatial and temporal slip distribution previously estimated<sup>14</sup> is used. Vertical and horizontal static seafloor deformations are calculated from the slip distribution assuming an elastic half space<sup>15</sup>. The delayed ruptures or the temporal slip distribution is also considered. The effects of the horizontal seafloor deformation on vertical sea surface deformation<sup>16</sup> are also included. For the bathymetric data, "Bottom topography data at 30 second grid around Japan" and "Basic Maps of the Sea in Coastal Waters" were compiled and provided by the Marine Information Research Center, Japan Hydrographic Association.

### Sediment threshold under the tsunami waves

An evaluation of the effect of the 2011 Tōhoku-Oki Tsunami waves on the sea floor were examined in terms of bottom current velocity of the waves. Because of their very long periods, tsunami waves are in effect shallow-water waves even in the deep ocean<sup>17</sup>. Therefore, velocities and directions of the simulated tsunami waves can be approximated to those near the sea floor. The maximum tsunami wave velocity and directions at each sampling station

were extracted from the results of the tsunami wave simulation. In order to calculate the critical velocity for grain entrainment, we applied Karman-Prandtl relationship between current velocity ( $U_z$ ) at a height  $z$  (we adopted 1 meter above the sea floor) and shear velocity ( $u_*$ ),

$$U_z = \frac{u_*}{\kappa} \ln \frac{z}{z_0} \quad (1)$$

where  $\kappa$  is von Karman's constant ( $\approx 0.41$ ) and  $z_0$  is the roughness length, and

$$z_0 = \left[ 1 - \exp\left(-\frac{u_* k_s}{28\nu}\right) + \frac{10\nu}{3u_* k_s} \right] \frac{k_s}{30} \quad (2)$$

where  $k_s = D_{50}$  (mean grain size) of the effective bed roughness and kinematic viscosity of sea water  $\nu = 1.31 \times 10^{-6} \text{ m}^2/\text{s}$ <sup>18</sup>.

Sediment particles on the sea floor could be entrained when shear velocity ( $u_*$ ) exceeds the critical threshold shear velocity ( $u_{*cr}$ ). The  $u_{*cr}$  for variable grain-sizes were derived through the Shields entrainment function  $\Theta_{cr}$  :

$$\Theta_{cr} = \frac{\rho u_{*cr}^2}{(\rho_s - \rho)gD} \quad (3)$$

where sediment density ( $\rho_s$ ) was taken as  $2650 \text{ kg/m}^3$  for rounded quartz–feldspathic grains;  $\rho$  was the density of seawater taken as  $1030 \text{ kg/m}^3$ ;  $D$  was the grain diameter (m). We used a fitted curve of the Shields diagram<sup>19</sup> to calculate the threshold Shields parameter  $\Theta_{cr}$  for cohesionless grains:

$$\Theta_{cr} = \frac{0.3}{1 + 1.2D_*} + 0.0055(1 - \exp[-0.020D_*]) \quad (4)$$

with dimensionless grain size :

$$D_* = \left( \frac{(\rho_s - \rho)g}{\nu^2} \right)^{1/3} D \quad (5)$$

We substituted variable silt- and sand-sized  $D$  into eqs. (3)–(5), and calculated  $u_{*cr}$  for each grain size. Then a threshold curve between current velocities and grain sizes was delineated by substituting  $u_{*cr}$  and  $D$  into eqs. (1) and (2). In regard to Typhoon Songda waves, we calculated the water velocities using wave heights and periods recorded at the the Mutsu-Ogawara tide gauge (141°23'14''E and 40°55'35''N). Their data is available to the public by the NOWPHAS (Nationwide Ocean Wave information network for Ports and HARbourS) database system run by the Ministry of Land, Infrastructure, Transport and Tourism (MLIT). The maximum wave height (11.41 m) and period (9.2 s) were recorded on the 30th May, 2011. The loci of water particle movement and water velocities induced by waves were calculated based on linear Airy wave theory<sup>18</sup>.

## References

- 1 Barnett, P. R. O., Watson, J. & Connelly, D. A multiple corer for taking virtually undisturbed samples from shelf, bathyal and abyssal sediments. *Oceanology* **7**, 399–408 (1984).
- 2 Schubert, C. J. & Nielsen, B. Effects of decarbonation treatments on  $d^{13}C$  values in marine sediments. *Mar. Chem.* **72**, 55–59 (2000).
- 3 Mayer, L. M. *et al.* Bioavailable amino acids in sediments: a biomimetic, kinetic-based approach. *Limnol. Oceanogr.* **40**, 511–520 (1995).
- 4 Rosenberg, W. *et al.* Liming effects on the chemical composition of the organic surface layer of a mature Norway spruce stand (*Picea abies* [L.] Karst.). *Soil Biol. Biochem.* **35**, 155–165 (2003).

- 5 Gremare, A. *et al.* Spatio-temporal changes in totally and enzymatically hydrolysable amino acids of superficial sediments from three contrasted areas. *Prog. Oceanogr.* **65**, 89–111 (2005).
- 6 Pastor, L. *et al.* Influence of the organic matter composition on benthic oxygen demand in the Rhône River prodelta (NW Mediterranean Sea). *Cont. Shelf Res.* **31**, 1008–1019 (2011).
- 7 Neveux, J. & Lantoiné, F. Spectrofluorometric assay of chlorophylls and phaeopigments using the least squares approximation technique. *Deep-Sea Res. Pt I* **40**, 1747–1765 (1993).
- 8 Walton, W. R. Techniques for recognition of living foraminifera. *Contr. Cushman Lab. Forum. Res.* **3**, 56–60 (1952).
- 9 Murray, J. W. & Bowser, S. S. Mortality, protoplasm decay rate, and reliability of staining techniques to recognise 'living' foraminifera: A review. *J. Foraminifer. Res.* **30**, 66–70 (2000).
- 10 Corliss, B. H. & Emerson, S. Distribution of rose bengal stained deep-sea benthic foraminifera from the Nova Scotian continental margin and Gulf of Maine. *Deep-Sea Res.* **37**, 381–400 (1990).
- 11 Bernhard, J. M. Distinguishing live from dead foraminifera: Methods review and proper applications. *Micropaleontology* **46 (Suppl. 1)**, 38–46 (2000).
- 12 Murray, J. W. *Ecology and Applications of Benthic Foraminifera*. (Cambridge University Press, 2006).
- 13 Satake, K., Nanayama, F. & Yamaki, S. Fault models of unusual tsunami in the 17th century along the Kuril trench. *Earth Planets Space* **60**, 925–935 (2008).

- 14 Satake, K., Fujii, Y., Harada, T. & Namegaya, Y. Time and space distribution of Coseismic slip of the 2011 Tohoku earthquake as inferred from tsunami waveform data. *B. Seismol. Soc. Am.* **103**, 1473-1492 (2013).
- 15 Okada, Y. Surface Deformation Due to Shear and Tensile Faults in a Half-Space. *B. Seismol. Soc. Am.* **75**, 1135-1154 (1985).
- 16 Tanioka, Y. & Satake, K. Tsunami generation by horizontal displacement of ocean bottom. *Geophys. Res. Lett.* **23** (1996).
- 17 Komar, P. D. *Beach Processes and Sedimentation*. 2nd edn, 544 (Prentice Hall, 1998).
- 18 Dade, W. B., Hogg, J. A. & Boudreau, B. P. in *The Benthic Boundary Layer: Transport Processes and Biogeochemistry* (eds B.P. Boudreau & B.B. Jørgensen) 4–43 (Oxford University Press, 2001).
- 19 Soulsby, R. *Dynamics of Marine Sands*. (Thomas Telford Publications, 1997).